

## Comparative immunohistochemistry of synaptic markers in the rodent hippocampus in pilocarpine epilepsy

Norbert Károly\*, András Mihály, Endre Dobó

Department of Anatomy, Faculty of Medicine, Szeged University, Kossuth L. sgt. 40, H-6724 Szeged, Hungary

### ARTICLE INFO

**Article history:**

Received 19 January 2010

Received in revised form 17 August 2010

Accepted 18 August 2010

**Keywords:**

Hippocampus

Mossy fibers

Pilocarpine

Seizures

Synaptic markers

Rats

Mice

### ABSTRACT

Pilocarpine-induced epileptic state (*Status epilepticus*) generates an aberrant sprouting of hippocampal mossy fibers, which alter the intrahippocampal circuits. The mechanisms of the synaptic plasticity remain to be determined. In our studies in mice and rats, pilocarpine-induced seizures were done in order to gain information on the process of synaptogenesis. After a 2-month survival period, changes in the levels of synaptic markers (GAP-43 and Syn-I) were examined in the hippocampus by means of semi-quantitative immunohistochemistry. Mossy fiber sprouting (MFS) was examined in each brain using Timm's sulphide-silver method. Despite the marked behavioral manifestations caused by pilocarpine treatment, only 40% of the rats and 56% of the mice showed MFS. Pilocarpine treatment significantly reduced the GAP-43 immunoreactivity in the inner molecular layer in both species, with some minor differences in the staining pattern. Syn-I immunohistochemistry revealed species differences in the sprouting process. The strong immunoreactive band of the inner molecular layer in rats corresponded to the Timm-positive ectopic mossy fibers. The staining intensity in this layer, representing the ectopic mossy fibers, was weak in the mouse. The Syn-I immunoreactivity decreased significantly in the hilum, where Timm's method also demonstrated enhanced sprouting. This proved that, while sprouted axons displayed strong Syn-I staining in rats, ectopic mossy fibers in mice did not express this synaptic marker. The species variability in the expression of synaptic markers in sprouted axons following pilocarpine treatment indicated different synaptic mechanisms of epileptogenesis.

© 2010 Elsevier GmbH. All rights reserved.

### 1. Introduction

The Pilocarpine Model of Epilepsy (PME) in rats and mice reproduces some of the features of human temporal lobe epilepsy (Nadler et al., 1980; Turski et al., 1984; Ben-Ari, 1985). A single dose of pilocarpine (PILO) acutely induces sequential behavioral changes indicative of an epileptic state (*Status epilepticus*) (SE) resulting in widespread damage to the forebrain in rodents (Turski et al., 1983). The acute period of the SE is followed by a silent (seizure-free) phase, which, lasts from 4 to 44 days. Morphological analysis confirms characteristic brain damage, including neuronal loss, glial proliferation and mossy fiber sprouting in the hippocampus (Mello et al., 1993). MFS occurs in the dentate gyrus (DG) of persons afflicted with medial temporal lobe epilepsy (MTLE). It involves

abnormal projections of mossy fibers (MF) to the internal molecular layer (IML) of the DG (de Lanerolle et al., 1989; Sutula et al., 1989; Masukawa et al., 1992). Similar sprouting characterizes the rodent model. Several weeks after pilocarpine-induced SE, new mossy fibers can be found in the CA3 region, the molecular layer and the hilum of the DG, by means of Timm's sulphide-silver method for zinc histochemistry (Mello et al., 1993). The axons that undergo MFS may form synapses, but their putative postsynaptic targets and microenvironment are obviously different in the hilum from in the molecular layer. By means of immunohistochemistry, we investigated possible neurochemical differences of the newly formed contacts.

One synaptic marker used to investigate synaptic remodelling, is neuromodulin or growth-associated phosphoprotein (GAP-43), a protein kinase C substrate (Lovinger et al., 1986). Expression of GAP-43 during embryonic growth (Casoli et al., 1996) and its re-expression in adults during attempted axonal regeneration, such as MFS, is well known (Benowitz et al., 1990). Developing neurons express high levels of GAP-43, which is transported to growth cones (Goslin et al., 1988). After the establishment of mature synaptic connections, GAP-43 levels decline in most neurons (Dani et al., 1991). The adult rodent hippocampus is one of the brain areas where GAP-43 persists, probably as a conse-

**Abbreviations:** DAB, diaminobenzidine; DG, dentate gyrus; GAP-43, growth-associated phosphoprotein; Glu, glutamate; IML, internal molecular layer; MF, mossy fiber; MFS, mossy fiber sprouting; MTLE, medial temporal lobe epilepsy; PB, phosphate buffer; PILO, pilocarpine; PME, Pilocarpine Model of Epilepsy; SE, *Status epilepticus*; SL, *Stratum lucidum*; Syn-I, synapsin I.

\* Corresponding author.

E-mail address: karolyno@anatomy.szote.u-szeged.hu (N. Károly).

quence of a high degree of synaptic structural plasticity (Casoli et al., 1996).

The other family of synaptic markers, the synapsins, consists of phosphoproteins associated with the cytoplasmic surface of the synaptic vesicle membranes (De Camilli et al., 1983). Synapsins are considered important in synaptic maturation and in the regulation of the release of neurotransmitters, including glutamate (Glu) (Greengard et al., 1993). The level of phosphorylation of synapsin I (Syn-I), a member of the synapsin family, increases under conditions that promote  $\text{Ca}^{2+}$ -dependent neurotransmitter release (Yamagata et al., 1995). This phosphorylation results in conformational changes in the Syn-I molecule, which promotes the availability of synaptic vesicles for exocytosis (Ceccaldi et al., 1995). An increase in Syn-I levels in response to injury and/or selected environmental stimuli is thought to lead to long-term excitability changes in a synaptic circuit (Greengard et al., 1993). It has been suggested that the increased amounts of Syn-I can be used as a marker of enhanced presynaptic activation (Melloni et al., 1994). The aim of the present experiments was to investigate these two synaptic markers in a model of MTLE, in rats and mice. The sprouting has also been detected by means of zinc histochemistry.

## 2. Materials and methods

### 2.1. Treatment

Adult male Wistar rats (220–300 g) and CFLP mice (Animal Husbandry Services, Domaszék, Hungary) (25–30 g) were injected intraperitoneally (i.p.) with 380 mg/kg and 190 mg/kg pilocarpine (PILO) (Sigma-Aldrich, St. Louis, MO, USA), respectively. Ninety minutes after the onset of the *Status epilepticus* (SE), the animals were injected with diazepam (Seduxen) (Richter Gedeon, Budapest, Hungary) (10 mg/kg, i.p.). The control animals received the same volume of physiological saline, the solvent of PILO.

### 2.2. Tissue preparation

The rats (6 control and 7 PILO-treated) and mice (7 control and 6 PILO-treated) were sacrificed 2 months after the injections. The animals were deeply anesthetized with diethyl-ether, perfused with 0.3% sodium sulphide in 0.1 M phosphate buffer (PB), and then fixed with 4% formaldehyde in phosphate buffer. The brains were cryoprotected with 30% sucrose, and sectioned on a freezing microtome at 24  $\mu\text{m}$ .

### 2.3. Timm's silver-sulphide method

Coronal-plane sections of the hippocampi were processed for Timm's staining (Timm, 1958; Danscher et al., 2004). The staining solution is composed of: 60 ml 50% gum arabic, 10 ml 2 M sodium citrate buffer, pH 3.7, 30 ml 5.67% hydroquinone, and 0.5 ml 17% silver nitrate solution. The sections were continuously agitated in a dark chamber for 50–60 min. The staining process was terminated with 2% sodium acetate, and the unreacted silver ions were removed with 5% sodium thiosulphate. The sections were mounted with DPX.

### 2.4. Immunohistochemistry

Coronal-plane tissue sections were treated with 0.5% Triton X-100 and 3% hydrogen peroxide for 10 min, and then with normal swine serum (1:10). The specimens were incubated with the primary antisera (rabbit anti-Syn-I; Chemicon, Temecula, CA, USA, 1:1000); mouse anti-GAP-43 (Sigma-Aldrich, St. Louis, MO, USA, 1:1000) at room temperature overnight. After this, the

sections were incubated with the appropriate biotinylated secondary antibody (1:500) (Jackson ImmunoResearch, West Grove, PA, USA) for 90 min, and finally with peroxidase-labelled streptavidin for 90 min. The sites of immunoreaction were visualized with the chromogen diaminobenzidine (DAB) tetrahydrochloride.

### 2.5. Image analysis

The pictures were taken by means of an image-capture system (Olympus DP50) attached to an Olympus BX-50 microscope and appropriate image analysis software (Soft Imaging System GmbH, Münster, Germany) and Adobe Photoshop 7 (Adobe Systems Inc., San Jose, CA, USA). The pixel density of immunoreactivity was determined in a blind study by a researcher unaware of the experimental treatment of the animals. Briefly: through use of the "marquee" tool, 8–12 circular selections in 0.1 mm diameter were made in immediately adjacent positions along the layers. The average of 10 background determinations (carried out near the layers of interest at neuropil sites not demonstrating positive staining) was subtracted from the average pixel densities measured within the hippocampal layers. Differences between the corresponding hippocampal regions of PILO-treated and control animals were assessed using the unpaired one-tailed Student's *t*-test. Data were analysed and plotted with the aid of GraphPad 4.0 (GraphPad Software, Inc., CA, USA). For every measurement, 8 hippocampal sections in the rat model and 12 sections in the mouse model were used in each animal.

## 3. Results

### 3.1. Seizure activity and behavior

Following PILO injection, the animals are expected to exhibit *Status epilepticus* (SE). In our experiments, one-third of the animals (regardless of the species), did not develop SE, and about half of those which did display SE, died during severe convulsions. Most of the injected animals demonstrated seizure symptoms of grade I–IV according to Racine et al. (1972). A few of the animals suffered grade V SE (Racine et al., 1972), with symptoms repeated for 1 h at least. These animals were injected with diazepam (10 mg/kg) in an effort to promote their survival. During the post-seizure period (2 months), many of the animals developed spontaneous seizures: stage IV or stage V symptoms were observed daily 1–2 weeks following the PILO treatment. These data correspond to descriptions in the literature (Cavalheiro, 1995). Aggressive behavior was frequently observed among the mice that reacted lastingly to PILO. These animals often fought each other causing wounds on the back and on the tail.

### 3.2. Timm's staining

Timm's staining is an accepted method for the visualization of zinc-containing neuronal elements (Kozma et al., 1981). Our observations concerning zinc histochemistry in the hippocampus are in good agreement with literature reports (Cavalheiro et al., 1996; Lemos and Cavalheiro, 1995). Briefly, Timm's staining demonstrated a high density of strongly stained varicose axons in the hilum and in the *Stratum lucidum* (SL), 40% of the PILO-treated rats and 56% of the PILO-treated mice exhibited increases in staining intensity in the areas described above. Sprouted mossy fibers in ectopic locations were detected in the supragranular layers of the DG and in the infrapyramidal layer of the CA3 region. These animals were termed "reacted", and used for further investigation by semi-quantitative immunohistochemical procedures during the present

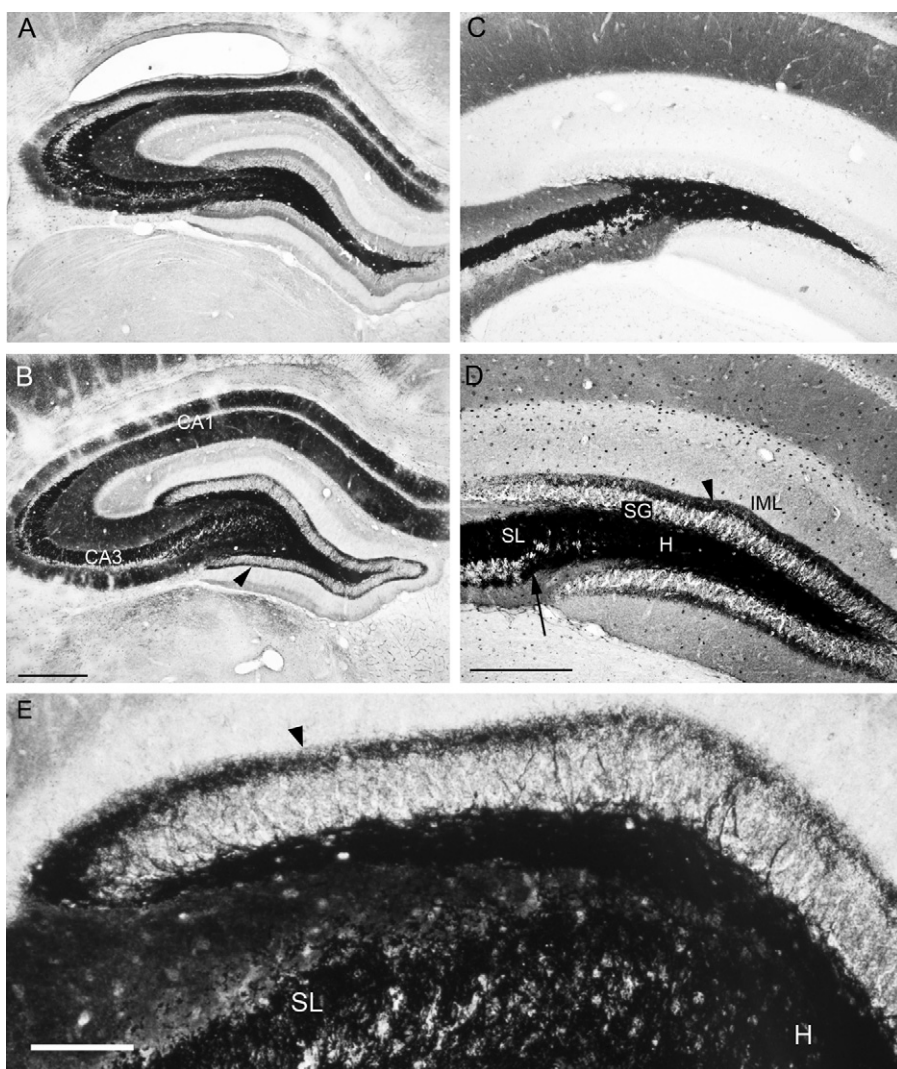


**Fig. 1.** Timm's staining after 2 months. (A) control rat, (B) PILO rat, (C) control mouse, (D) PILO mouse, and (E) PILO rat. Demonstration of aberrant sprouting in the SG layer of the IML (arrowhead) and infrapyramidal layer (arrow) of a PILO-treated mouse and rat revealed by means of Timm's staining. IML, inner molecular layer; SL, stratum lucidum; H, hilum; SG, supragranular layer. Scale bars in A and B = 0.5 mm; C and D = 200 µm; E = 125 µm.

study. Species differences in staining patterns and intensities were not found in the “reacted” group (Fig. 1).

### 3.3. GAP-43 immunohistochemistry

The picture of hippocampal GAP-43 immunostaining was similar in the two rodent species with, the most intense immunoreactivity in the *Stratum lacunosum-moleculare* (Fig. 2) and somewhat less, but still strong and homogeneous staining, in the IML of the DG in both species. The polymorphic layer of the DG and the SL of the CA3 field were devoid of staining. The principal neurons did not stain.

#### 3.3.1. Mouse

In the PILO-treated animals, the extent of staining of the IML was significantly reduced relative to the controls (mouse: 40%; rat: 34%) (Figs. 2C, D and 3A). No differences were noted between the control and PILO-treated animals in other hippocampal layers.

#### 3.3.2. Rat

GAP-43 immunohistochemistry revealed a significant reduction in the staining intensity of the IML (Figs. 2A, B and 3B). In contrast with the mouse, the IML of the rat was not a homogeneously

stained band but displayed a middle sub-layer, where the GAP-43 immunoreactivity was reduced (Fig. 2B and D).

### 3.4. Syn-I immunohistochemistry

Strong immunoreactivity for Syn-I was found in the mossy fibers in both rodents (Fig. 4). The cell bodies were not labelled. The molecular layer was moderately positive.

#### 3.4.1. Mouse

After 2 months PILO treatment, the density of labelled elements in the SL was increased significantly (Figs. 4D and 5A). Moreover, the layer displaying Syn-I immunostaining thickened considerably. The dentate hilum, which also contained mossy fiber terminals, as verified by Timm's staining, exhibited a highly significantly decreased staining intensity of Syn-I (Figs. 1 and 4D). In the IML, the overall staining did not change significantly, though a weak immunoreactive band appeared in the innermost supragranular layer (Figs. 4C, D and 5A).

#### 3.4.2. Rat

Analysis of the brain sections from the PILO-treated and the control animals revealed both similarities and differences to the

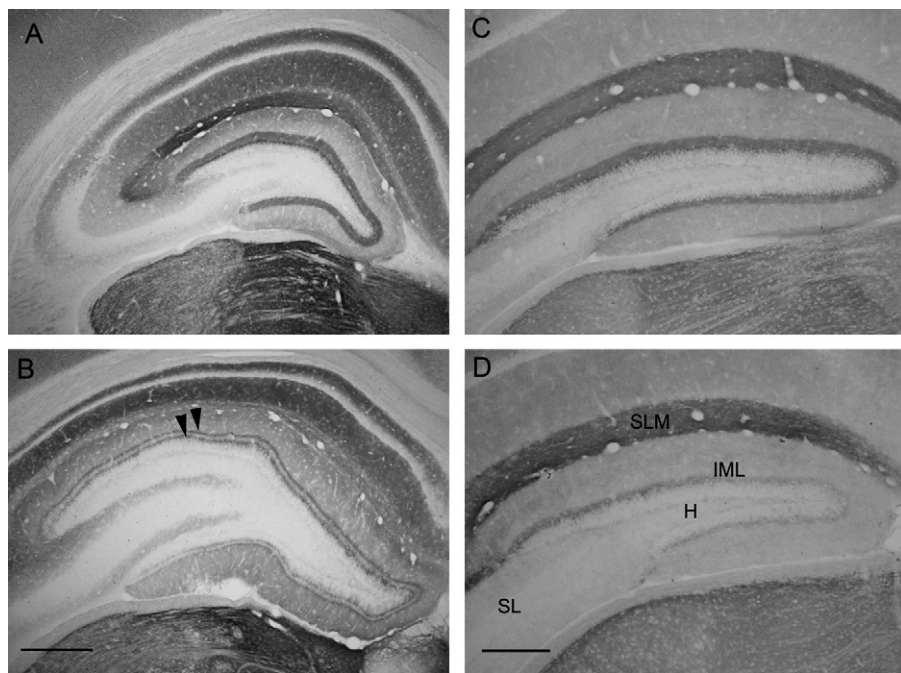


**Fig. 2.** Immunolocalization of GAP-43 after 2 months. (A) Control rat, (B) PILO rat, (C) control mouse and (D) PILO mouse. The GAP-43-positive band in the IML is thicker in the control animals while in the PILO-reacted rodents show paler bands furthermore the rat displays two thin bands (arrowheads). The most intense immunoreactivity was observed in the *Stratum lacunosum-moleculare*. IML, inner molecular layer; SL, *Stratum lucidum*; H, hilum; SLM, *Stratum lacunosum-moleculare*. Scale bars in A and B = 0.5 mm; C and D = 200  $\mu$ m.

mouse (Figs. 4 and 5). The PILO-induced seizures enhanced the Syn-I immunoreactivity significantly in every layer (Figs. 4B and 5B), including the hilum, which was much more weakly immunolabelled in the mouse. Nevertheless, an extra Syn-I-IR band appeared in the IML, in the supragranular zone of the ectopic mossy fibers. The staining pattern in the PILO-treated rat resembled that of Timm's staining, indicating that this synaptic marker protein had accumulated in the sprouted mossy fibers. Table 1 summarizes the alterations in immunostaining in the measured hippocampal regions of the PILO-treated animals.

#### 4. Discussion

##### 4.1. Timm's staining

MFS has been previously detected in the epileptic hippocampus by means of Timm's method (Lemos and Cavalheiro, 1995; Cavalheiro et al., 1996; Jiao and Nadler, 2007). Our data are in agreement with the reports in the literature and corroborate the increased density of mossy fibers in the SG layer, hilum of the DG, and the SL of the CA3 region. Zinc is localized in the synap-

tic vesicles of Glu-ergic granule cell axons (Paoletti et al., 2009), and MFS increases the amount of zinc liberated during synaptic activity. It should be emphasized that zinc detected by Timm's staining is present not only in the giant mossy terminals, but also in the thin granule cell axons (Seress et al., 2001), indicating that Timm-positivity is not a specific marker for the mossy terminals. Zinc exerts pharmacological effects locally on NMDA receptors and Glu transporters (Paoletti et al., 2009). Nevertheless, whether zinc is a proconvulsant (Pei et al., 1983) or an anticonvulsant agent remains unclear (Williamson and Spencer, 1995; Paoletti et al., 2009).

##### 4.2. GAP-43 immunohistochemistry

The staining pattern of the GAP-43 protein in our control animals conforms to the data in the literature (Tolner et al., 2003). We found that GAP-43 immunoreactivity of the IML in the PILO-reacted animals decreased significantly, which is in line with the after-seizure down-regulation of GAP-43 expression in the IML (Tolner et al., 2003; Borges et al., 2004; Longo et al., 2005). Other studies have reported the upregulation of this protein after kainic acid treatment

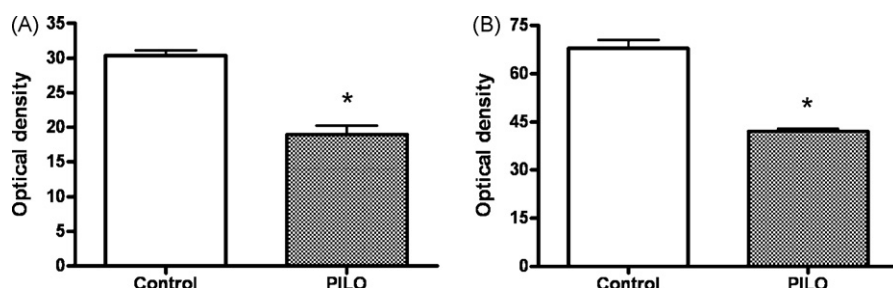


**Fig. 3.** Densitometry of GAP-43. GAP-43 immunoreactivity in the PILO-reacted mouse IML (A), GAP-43 immunoreactivity in the PILO-reacted rat IML (B). The density of the GAP-43-positive band was significantly higher for the controls than for PILO-treated animals among both rodents ( $p < 0.0001$ ).

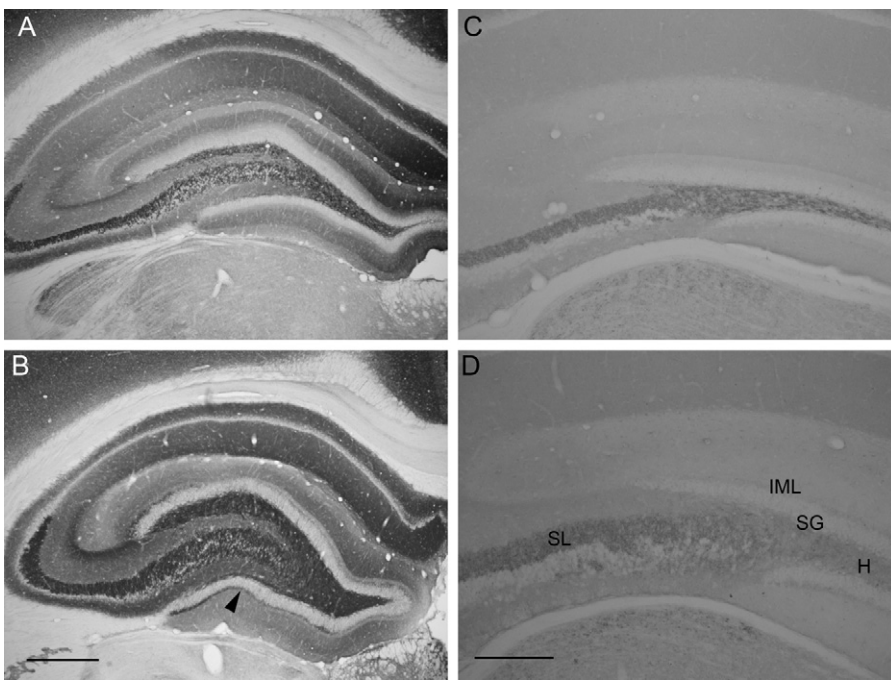


**Fig. 4.** Immunolocalization of Syn-I after 2 months. (A) Control rat, (B) PILO rat, (C) control mouse and (D) PILO mouse. The decreased immunoreactivity is readily visible in the H and the increased IR in the SL among the PILO-reacted mice (D) while increased in every measured field among the rats. In addition an extra Syn-I-IR band (arrowhead) appeared in the IML, in the supragranular zone of the ectopic mossy fibers (B). IML, inner molecular layer; SL, Stratum lucidum; H, hilum; SG, supragranular cell layer. Scale bars in A and B = 0.5 mm; C and D = 200  $\mu$ m.

(McNamara and Routtenberg, 1995), kindling (Dalby et al., 1995) or PILO seizures (Naffah-Mazzacoratti et al., 1999). In embryonic stem cell cultures, GAP-43 production was restricted to a separate axonal compartment (Mundigl et al., 1993). GAP-43 is also expressed transiently in the dendrites, but the main localization sites are in the axonal growth cones (Goslin and Banker, 1990). GAP-43 is a presynaptic protein (Skene et al., 1986; Meiri and Gordon-Weeks, 1990). However, it has not yet been established with certainty that GAP-43 remains in the axon terminals after the sprouting process has finished. Our results suggest that GAP-43 may disappear from the mossy fiber terminals after they establish synapses.

No change in GAP-43 staining relative was noticed in the molecular layer of the DG in human non-sclerotic, epileptic hippocampi to the control brain samples (Proper et al., 2000). On the other hand, in epilepsy cases with serious hippocampal sclerosis, the GAP-43 level was elevated in the SG layer of the DG (Proper et

al., 2000). In the present study, the PILO-treated animals featuring ectopic supragranular MFS ("reacted mice"), did not exhibit the typical morphological hallmarks of hippocampal sclerosis, as assessed from subsequent sections, which were immunostained with the neuron-specific anti-NeuN antibody (data not shown). There was a considerable loss in GAP-43 immunostaining in the IML of reacted mice and rats. In rats, the loss of the larger middle band of the IML may be accounted for by the degeneration of mossy cells, the vulnerability of which to PILO treatment has been documented (Longo et al., 2003). It is difficult to explain the presence of the outermost (towards the periphery of the DG) separate narrow immunostained band. In the PILO-treated samples, there was a homogeneous reduction in CGRP-containing axon density in the IML (Scharfman et al., 2001). Therefore, this "extra" band may be composed either of sprouted axons of surviving aberrant mossy cells (Scharfman et al., 2001) or growing axons of unknown ori-

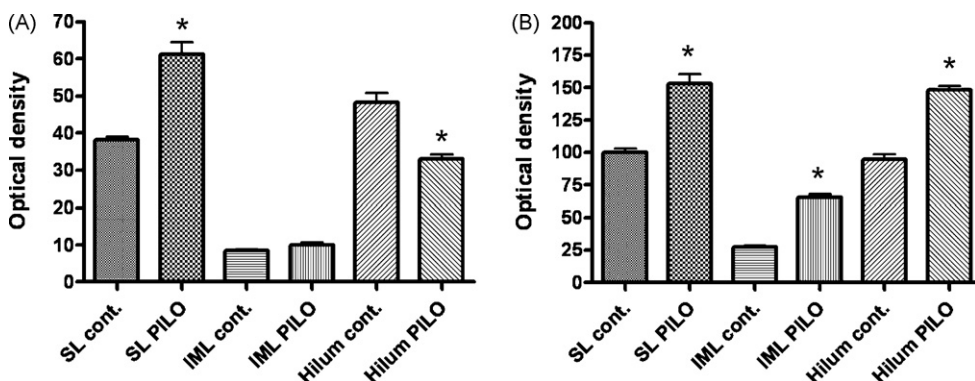


**Fig. 5.** Densitometry of Syn-I immunoreactivity in the mouse and rat. (A) Comparison of measured hippocampal regions in the mouse showing significant changes between SL control and SL PILO ( $p < 0.0001$ ) and between H control and H PILO ( $p < 0.0001$ ). There were no measurable changes between the reacted and the control IML. (B) In the rats the PILO-induced seizures significantly enhanced the Syn-I IR in every layer: SL cont vs. SL PILO ( $p = 0.0005$ ), IML cont vs. IML PILO ( $p < 0.0001$ ) and H cont vs. H PILO ( $p < 0.0001$ ) IML, inner molecular layer; SL, Stratum lucidum; H, hilum.

**Table 1**

Changes of synaptic markers (Syn-I, GAP-43 and Zn content) in the most effected layers of the mouse and rat hippocampi. The upward arrows show significant increase, the downward arrows indicate decrease in the appropriate layers. Note that Syn-I IR changes in the opposed directions in the mouse and rat hilas.

	Hilum	SL	IML
Syn-I IR	Mouse ↓, Rat ↑	Mouse ↑, Rat ↑	Mouse no change, Rat ↑ <sup>(a)</sup>
GAP-43 IR	No change	No change	Mouse ↓, Rat ↓
Timm-staining	Mouse ↑, Rat ↑	Mouse ↑, Rat ↑, and IP also <sup>(b)</sup>	Mouse ↑, Rat ↑

<sup>a</sup> An extra Syn-I-IR band appeared in the IML.

<sup>b</sup> Massive staining appeared in the infrapyramidal layer (IP) in mossy fiber terminal fields originating from the dentate gyrus.

gin (including inhibitory local or septal projection cells (Duvernoy, 2005). Thus, we presume that this external GAP-43-stained band is not directly related to the sprouted mossy fibers.

#### 4.3. Syn-I immunohistochemistry

The presence of the Syn-I protein in mossy fiber terminals is a well-known feature of the adult rodent brain (De Camilli et al., 1983). The high Syn-I mRNA levels in the DG correlates with the increased Syn-I protein expression in the SL of the CA3 region, pointing to the importance of the axonal transport of Syn-I from the granule cell to the mossy fiber axon terminals (Zurmohle et al., 1994). In the epileptic rats, the Syn-I staining was increased similarly to the Timm-positivity. The hilum, the SL of the CA3 region and the IML of the DG displayed significant increases. Mice reacted to PILO differently, only the SL displaying an increase in Syn-I staining. The immunoreactivity in the hilum decreased, and the IML did not undergo any change. These results suggest that in rats the MFS may be accompanied by enhanced Glu release (Mitsuya et al., 2009) in the hilum, SL and IML, while in mice (supposing no species-specific differences in the functions of hippocampal Syn-I in the rodents) the MFS in some of these regions resulted in silent synapses: functional synapses with increased Glu release apparently occurred only in the SL. Alternatively, the coincidence of the increased amount of zinc and the decreased Syn-I immunoreactivity in the hilum and in the IML may indicate strong inhibition counterbalancing the MFS in these regions. There are reports in the literature which point to the possibility that the Glu-ergic hilar and IML axons are inhibited more effectively in mice than in rats (Nadler et al., 2007).

We conclude that the changes in Syn-I immunoreactivity correlate well with MFS in rats, but not in mice. GAP-43-associated synaptogenesis is not an essential component of the MFS in PILO-induced seizures in either species, but rather occurs in surviving aberrant mossy cells, or sprouting axons of unknown nerve cells. Our data indicate fundamental inter-species differences, that need to be considered when the experimental results are extrapolated. Great individual variability was found in the susceptibility to epileptic factors. Therefore the application of Timm's staining is suggested in the future studies as a control morphological tool before interpretation of the results, in order to validate those animals for further investigations, which not only reacted to PILO injection with immediate behavioral changes, but also manifest MFS.

#### References

- Ben-Ari Y. Limbic seizure and brain damage produced by kainic acid: mechanisms and relevance to human temporal lobe epilepsy. *Neuroscience* 1985;14:375–403.
- Benowitz LI, Rodriguez WR, Neve RL. The pattern of GAP-43 immunostaining changes in the rat hippocampal formation during reactive synaptogenesis. *Brain Res Mol Brain Res* 1990;8:17–23.
- Borges K, McDermott DL, Dingledine R. Reciprocal changes of CD44 and GAP-43 expression in the dentate gyrus inner molecular layer after status epilepticus in mice. *Exp Neurol* 2004;188:1–10.
- Casoli T, Spagna C, Fattoretti P, Gesuita R, Bertoni-Freddari C. Neuronal plasticity in aging: a quantitative immunohistochemical study of GAP-43 distribution in discrete regions of the rat brain. *Brain Res* 1996;714:111–7.
- Cavalheiro EA. The pilocarpine model of epilepsy. *Ital J Neurol Sci* 1995;16:33–7.
- Cavalheiro EA, Santos NF, Priel MR. The pilocarpine model of epilepsy in mice. *Epilepsia* 1996;37:1015–9.
- Ceccaldi PE, Grohovaz F, Benfenati F, Chieregatti E, Greengard P, Valtorta F. Dephosphorylated synapsin I anchors synaptic vesicles to actin cytoskeleton: an analysis by videomicroscopy. *J Cell Biol* 1995;128:905–12.
- Dalby NO, Rondouin G, Lerner-Natoli M. Increase in GAP-43 and GFAP immunoreactivity in the rat hippocampus subsequent to perforant path kindling. *J Neurosci Res* 1995;41:613–9.
- Dani JW, Armstrong DM, Benowitz LI. Mapping the development of the rat brain by GAP-43 immunocytochemistry. *Neuroscience* 1991;40:277–87.
- Danscher G, Stoltzenberg M, Bruhn M, Sondergaard C, Jensen D. Immersion autometallography: histochemical in situ capturing of zinc ions in catalytic zinc-sulfur nanocrystals. *J Histochem Cytochem* 2004;52:1619–25.
- De Camilli P, Cameron R, Greengard P. Synapsin I (protein I), a nerve terminal-specific phosphoprotein. I. Its general distribution in synapses of the central and peripheral nervous system demonstrated by immunofluorescence in frozen and plastic sections. *J Cell Biol* 1983;96:1337–54.
- de Lanerolle NC, Kim JH, Robbins RJ, Spencer DD. Hippocampal interneurone loss and plasticity in human temporal lobe epilepsy. *Brain Res* 1989;495:387–95.
- Duvernoy H. Structure, functions, and connections. In: Duvernoy H, editor. *The human hippocampus*. 3rd ed. Berlin Heidelberg: Springer; 2005. p. 5–37.
- Goslin K, Schreyer DJ, Skene JH, Banker G. Development of neuronal polarity: GAP-43 distinguishes axonal from dendritic growth cones. *Nature* 1988;336:672–4.
- Goslin K, Banker G. Rapid changes in the distribution of GAP-43 correlate with the expression of neuronal polarity during normal development and under experimental conditions. *J Cell Biol* 1990;110:1319–31.
- Greengard P, Valtorta F, Czernik AJ, Benfenati F. Synaptic vesicle phosphoproteins and regulation of synaptic function. *Science* 1993;259:780–5.
- Jiao Y, Nadler JV. Stereological analysis of GluR2-immunoreactive hilar neurones in the pilocarpine model of temporal lobe epilepsy: correlation of cell loss with mossy fibre sprouting. *Exp Neurol* 2007;205:569–82.
- Kozma M, Szerdahelyi P, Kasa P. Histochemical detection of zinc and copper in various neurones of the central nervous system. *Acta Histochem* 1981;69:12–7.

- Lemos T, Cavalheiro EA. Suppression of pilocarpine-induced status epilepticus and the late development of epilepsy in rats. *Exp Brain Res* 1995;102:423–8.
- Longo B, Covolan L, Chadi G, Mello LE. Sprouting of mossy fibres and the vacating of postsynaptic targets in the inner molecular layer of the dentate gyrus. *Exp Neurol* 2003;181:57–67.
- Longo B, Vezzani A, Mello LE. Growth-associated protein 43 expression in hippocampal molecular layer of chronic epileptic rats treated with cycloheximide. *Epilepsia* 2005;46(Suppl 5):125–8.
- Lovinger DM, Colley PA, Akers RF, Nelson RB, Routtenberg A. Direct relation of long-term synaptic potentiation to phosphorylation of membrane protein F1, a substrate for membrane protein kinase C. *Brain Res* 1986;399:205–11.
- Masukawa LM, Urano K, Sperling M, O'Connor MJ, Burdette LJ. The functional relationship between antidromically evoked field responses of the dentate gyrus and mossy fibre reorganization in temporal lobe epileptic patients. *Brain Res* 1992;579:119–27.
- McNamara RK, Routtenberg A. NMDA receptor blockade prevents kainate induction of protein F1/GAP-43 mRNA in hippocampal granule cells and subsequent mossy fibre sprouting in the rat. *Brain Res Mol Brain Res* 1995;33:22–8.
- Meiri KF, Gordon-Weeks PR. GAP-43 in growth cones is associated with areas of membrane that are tightly bound to substrate and is a component of a membrane skeleton subcellular fraction. *J Neurosci* 1990;10:256–66.
- Mello LE, Cavalheiro EA, Tan AM, et al. Circuit mechanisms of seizures in the pilocarpine model of chronic epilepsy: cell loss and mossy fibre sprouting. *Epilepsia* 1993;34:985–95.
- Melloni Jr RH, Apostolidis PJ, Hamos JE, DeGennaro LJ. Dynamics of synapsin I gene expression during the establishment and restoration of functional synapses in the rat hippocampus. *Neuroscience* 1994;58:683–703.
- Mitsuya K, Nitta N, Suzuki F. Persistent zinc depletion in the mossy fibre terminals in the intrahippocampal kainate mouse model of mesial temporal lobe epilepsy. *Epilepsia* 2009;50:1979–90.
- Mundigl O, Matteoli M, Daniell L, et al. Synaptic vesicle proteins and early endosomes in cultured hippocampal neurones: differential effects of Brefeldin A in axon and dendrites. *J Cell Biol* 1993;122:1207–21.
- Nadler JV, Perry BW, Cotman CW. Selective reinnervation of hippocampal area CA1 and the fascia dentata after destruction of CA3–CA4 afferents with kainic acid. *Brain Res* 1980;182:1–9.
- Nadler JV, Tu B, Timofeeva O, Jiao Y, Herzog H. Neuropeptide Y in the recurrent mossy fibre pathway. *Peptides* 2007;28:357–64.
- Naffah-Mazzacoratti MG, Funke MG, Sanabria ER, Cavalheiro EA. Growth-associated phosphoprotein expression is increased in the supragranular regions of the dentate gyrus following pilocarpine-induced seizures in rats. *Neuroscience* 1999;91:485–92.
- Paoletti P, Vergnano AM, Barbour B, Casado M. Zinc at glutamatergic synapses. *Neuroscience* 2009;158:126–36.
- Pei Y, Zhao D, Huang J, Cao L. Zinc-induced seizures: a new experimental model of epilepsy. *Epilepsia* 1983;24:169–76.
- Proper EA, Oestreicher AB, Jansen GH, et al. Immunohistochemical characterization of mossy fibre sprouting in the hippocampus of patients with pharmaco-resistant temporal lobe epilepsy. *Brain* 2000;123(Pt 1):19–30.
- Racine RJ, Gartner JG, Burnham WM. Epileptiform activity and neural plasticity in limbic structures. *Brain Res* 1972;47:262–8.
- Scharfman HE, Smith KL, Goodman JH, Sollas AL. Survival of dentate hilar mossy cells after pilocarpine-induced seizures and their synchronized burst discharges with area CA3 pyramidal cells. *Neuroscience* 2001;104:741–59.
- Seress L, Abraham H, Paleszter M, Gallyas F. Granule cells are the main source of excitatory input to a subpopulation of GABAergic hippocampal neurones as revealed by electron microscopic double staining for zinc histochemistry and parvalbumin immunocytochemistry. *Exp Brain Res* 2001;136:456–62.
- Skene JH, Jacobson RD, Snipes GJ, McGuire CB, Norden JJ, Freeman JA. A protein induced during nerve growth (GAP-43) is a major component of growth-cone membranes. *Science* 1986;233:783–6.
- Sutula T, Cascino G, Cavazos J, Parada I, Ramirez L. Mossy fibre synaptic reorganization in the epileptic human temporal lobe. *Ann Neurol* 1989;26:321–30.
- Timm F. Zur Histochemie der Schwermetalle. Das Sulfid-Silberverfahren. *Dtsch Z Gerichtl Med* 1958;46:706–11.
- Tolner EA, van Vliet EA, Holtmaat AJ, Aronica E, Witter MP, da Silva FH, Gorter JA. GAP-43 mRNA and protein expression in the hippocampal and parahippocampal region during the course of epileptogenesis in rats. *Eur J Neurosci* 2003;17:2369–80.
- Turski WA, Czuczwar SJ, Kleinrok Z, Turski L. Cholinomimetics produce seizures and brain damage in rats. *Experientia* 1983;39:1408–11.
- Williamson A, Spencer D. Zinc reduces dentate granule cell hyperexcitability in epileptic humans. *Neuroreport* 1995;6:1562–4.
- Turski WA, Cavalheiro EA, Bortolotto ZA, Mello LM, Schwarz M, Turski L. Seizures produced by pilocarpine in mice: a behavioral, electroencephalographic and morphological analysis. *Brain Res* 1984;321:237–53.
- Yamagata Y, Obata K, Greengard P, Czernik AJ. Increase in synapsin I phosphorylation implicates a presynaptic component in septal kindling. *Neuroscience* 1995;64:1–4.
- Zurmohle UM, Herms J, Schlingensiepen R, Schlingensiepen KH, Brysch W. Changes of synapsin I messenger RNA expression during rat brain development. *Exp Brain Res* 1994;99:17–24.